Requirements for oversized holes for reusable steel-concrete composite floor systems

Nijgh, M.P.(Martin); Veljkovic, M. (Milan)

DOI
10.1016/j.istruc.2020.01.021

Publication date
2020

Document Version
Final published version

Published in
Structures

Structures 24 (2020) 489–498

Contents lists available at ScienceDirect

Structures

journal homepage: www.elsevier.com/locate/structures

Requirements for oversized holes for reusable steel-concrete composite floor systems

M.P. (Martin) Nijgh*, M. (Milan) Veljkovic

Faculty of Civil Engineering and Geosciences, Delft University of Technology, Delft, The Netherlands

ARTICLE INFO

Keywords:
Sustainability
Composite floor system
Deviation
Resin-injected bolted connection
Bearing strength

ABSTRACT

The design of sustainable structures is increasingly gaining attention in the construction sector as a societal and technological challenge. Demountability and reuse of structures contributes to the reduction of the environmental impact of the built environment. Welded headed studs used in traditional steel-concrete composite floor systems need to be replaced by demountable shear connectors to enable the transition of the construction sector to a circular business model. The demountable shear connectors are embedded in large prefabricated concrete floor elements and connected to steel beams by bolts. The holes in the beam flange are oversized to account for geometrical and dimensional deviations of all members and to facilitate rapid execution and easy demounting. The goal of this paper is to present a methodology that quantifies the required nominal hole clearance for reusable composite floor systems. Statistical characteristics of dimensional and geometrical deviations serve as input for Monte-Carlo simulations. The aggregated results of the Monte Carlo simulations are used to determine the required nominal hole clearance for a specified probability of successful installation of the demountable shear connectors. The proposed methodology is applied to the composite floor system of a demountable and reusable car park building. The contradicting requirement of oversized holes and composite interaction is solved by injecting the hole clearance with a (steel-reinforced) epoxy resin. The bearing resistance of the (steel-reinforced) epoxy resin is addressed based on preliminary results of creep experiments on resin-injected bolted connections.

1. Introduction

Environmental concerns steer the construction industry towards the development of more sustainable structural alternatives. Steel frame structures allow for disassembly and the subsequent recovery and reuse or recycling of the steel members. However, the disassembly of traditional steel-concrete composite floor systems is impaired by non-demountable welded headed studs, which increase the load bearing resistance and decreases the deformations by providing composite interaction. Applying demountable shear connectors (e.g. [1–4]) in combination with large prefabricated concrete floor elements allows for the reuse of a structure by (i) changing the floor plan to allow for different functional use or (ii) by re-assembling the structure at another location. By designing for reusability, the lifetime of the structure is no longer controlled by its functional lifetime, but by its technical lifetime [5].

Tingly & Davison [6] indicate that, amongst other factors, composite construction and longer (dis)assembly times are the main barriers in the widespread development and use of demountable and reusable composite floor systems. By identifying and quantifying the sources and effects of geometrical and dimensional deviations on the (dis)assembly process, the perceived risks of constructing demountable and reusable structures can be mitigated.

All engineering structures contain a degree of uncertainty with respect to their geometry. The magnitude of the uncertainty is controlled by imposing limits related to dimensional or geometrical deviations. Dimensional deviations concern the variation of a given dimension at a fixed point in space, whereas geometrical deviations are related to the variation of positions. The magnitude of the dimensional and geometrical deviations affect the speed of execution, the appearance, and the load bearing resistance of a structure. An extensive list of maximum deviations (tolerances) is specified in Annex B of EN 1090-2 [7], in which distinction is made between essential and functional tolerances. Essential tolerances are specified to ensure the validity of the design assumptions concerning resistance and stability, whereas functional tolerances are imposed to ensure executability and/or appearance. In this paper, tolerances are defined as the allowable difference and deviations are defined as the actual difference of a certain dimension or geometry.

* Corresponding author.
E-mail address: M.P.Nijgh@tudelft.nl (M.P.M. Nijgh).

https://doi.org/10.1016/j.istruc.2020.01.021
Received 22 November 2019; Received in revised form 16 January 2020; Accepted 18 January 2020

Table 1
Nominal hole clearances (mm) for bolted steel-to-steel connections according to EN 1090–2 [7].

Nominal bolt diameter d (mm)	12	14	16	18	20	22	24	27 and over
Normal round holes	1		2					3
Oversized round holes	3		4				6	8
Short slotted holes (on length)	4		6				8	10
Long slotted holes (on length)	1,5 x bolt diameter							

The functional tolerances specified in Annex B of EN 1090-2 [7] provide sufficient certainty that the various structural elements of a typical steel structure can be assembled using the nominal hole clearances for normal round holes specified in EN 1090-2 [7], see Table 1. The nominal hole clearance is defined as the difference between the nominal hole diameter and the nominal bolt diameter. In case of a complex structural design characterised by potential execution challenges, the contractor could preassemble the structure in the factory. Alternatively, the structure could be designed with connections with oversized round holes or slotted holes (see Table 1) to increase the probability of successful execution of the bolted connections. The latter is often the less expensive solution, because it saves the labour costs and time related to preassembly and because it can easily be implemented in the existing fabrication process. For the same reasons, this approach could also be the preferred option in case of demountable and reusable steel-concrete composite floor systems.

Recently, Nijgh et al. [4] successfully assembled and disassembled the main girder of a demountable and reusable composite floor system representing a part of a multi-storey car park building. The composite floor system consisted of three tapered steel beams with a span of 14.4 m, four prefabricated concrete floor elements (7.2 × 2.6 m) and M20 demountable shear connectors at a centre-to-centre distance of 300 mm. The magnitude of the hole clearances to facilitate rapid execution and easy demounting was quantified experimentally. The nominal hole clearances for successful installation of the composite floor system were significantly larger (12 mm) compared to the nominal clearances specified in Table 1. The tapered steel beams were braced at five locations along their span, reducing their out-of-straightness, which had a beneficial effect the observed geometrical deviations. On the other hand, the prefabricated floor elements used in the experiments [4] exhibited relatively large geometrical and dimensional deviations [8], which is discussed later in this paper.

According to Whitney [9], determining the character of the product or system is the first step in product design when optimising its (dis) assembly process. Secondly, a function analysis should be carried out, followed by a design-for-producibility-and-usability study. Based on the first three stages, the assembly process can be designed. Finally, the production system should be designed such that it is integrated with the supply of materials and with the customer demand. Whitney's approach is frequently used in the field of user product design, process innovation, automotive and IT, but no significant implementation exists in the construction sector. An overview of potential criteria of Whitney's five-step design concept [9] for demountable and reusable composite floor systems is introduced in Table 2.

Steps 1 and 2 of Whitney's models consists mostly of qualitative criteria, which may seem trivial but are relevant as they force designers and engineers to consider any potential problems ahead. Mitigating the perceived risks [6] of assembling and disassembling steel-concrete composite floor systems is the first stage to move past steps 1 and 2 towards potential implementation of the proposed floor system in practice.

This paper focuses on step 3 and 4 of Whitney's design process, with the main goal to quantify the nominal hole clearance that is required to rapidly assemble and easily disassemble steel-concrete composite floor systems. The current rules for detailing connections with oversized holes according to EN 1993-1-8 [10] are presented. A methodology to quantify the required nominal hole clearance for reusable composite floor systems is derived based on a specified probability of successful installation of the demountable shear connectors. A technical solution is discussed to solve the contradicting requirement of oversized holes required for (rapid) execution and normal clearance holes required for instantaneous composite interaction during the functional lifetime.

2. Geometrical and dimensional deviations

The alignment of the demountable shear connectors embedded in a prefabricated concrete floor element and the bolt holes in a steel beam depends on the geometrical and dimensional deviations of both members, as well as on the deviations within the structural grid. EN 1090-2 [7] contains an extensive list of maximum dimensional and geometrical deviations for two tolerance classes, with stricter requirements for tolerance class 2 compared to tolerance class 1. An overview of the governing geometrical and dimensional deviations is presented in this section. Distinction between deviations in various directions is made according to the global coordinate system shown in Fig. 1.

Table 2
Whitney's five-step design process [9] applied to demountable and reusable composite floor systems.

Step	Task [9]	Potential criteria for demountable and reusable composite floor systems
1	Determining the character of the product	• Complying with existing design codes. • Suitable for non-destructive disassembly • Sufficiently durable to last multiple lifecycles.
2	Identifying the function of the product	• Providing accommodation, office area, parking places, et cetera during the full technical lifetime of the structural elements.
3	Carrying out a design-for-producibility-and-usability study	• Accounting for the dimensional and geometrical deviations of the structural elements to facilitate a rapid assembly and disassembly phase. • Providing adaptability, i.e. an office building that can be converted to housing • Producing standardised structural elements to minimise errors and to optimise the production output.
4	Designing a (dis)assembly process	• Competitive in terms of time and costs compared to traditional (non-demountable) floor systems • Repetitive construction sequence • Standardised structural details (shear connection)
5	Designing a factory system	• Operating on minimal inventory • Not relying on scarce materials • Capability of producing the structural elements required for one building in short time • Traceability of the structural elements (e.g. element passport)

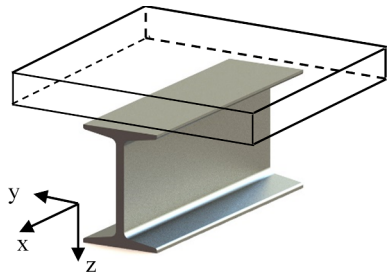

Fig. 1. Global coordinate system of the composite floor system.

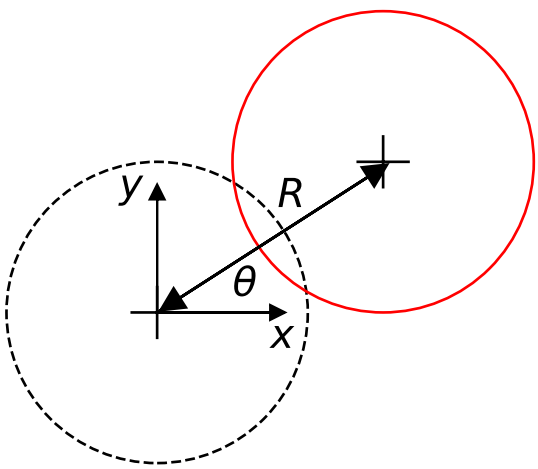

Fig. 2. Deviation of the actual hole position (red) from its nominal position (black). (For interpretation of the references to colour in this figure legend, the reader is referred to the web version of this article.)

2.1. Geometrical deviation of the location of bolt holes

It is assumed that the distance between the nominal and actual bolt hole location is represented by a random variable R, see Fig. 2. The direction in which this deviations occurs is controlled by random variable θ. The deviation along the axes of the coordinate system can then be expressed as

$$(\Delta x_{\text{hole}}, \Delta y_{\text{hole}}) = (R\cos\theta, R\sin\theta). \tag{1}$$

The magnitude of the deviation between the centreline of the bolt hole from its nominal position (R) is limited by EN 1090–2 [7] as ± 2 mm and ± 1 mm for tolerance class 1 and 2, respectively.

2.2. Out-of-straightness of the beam

The initial out-of-straightness of the steel beams affects the probability of transversal alignment of the bolt holes in the top flange and the demountable shear connectors embedded in the prefabricated concrete floor elements. Generally, the out-of-straightness of beams and columns is represented by a half sine wave with imperfection amplitude $A_{0,u}$, expressed by

$$\Delta y_{\text{str,u}} = A_{0,u}\sin\left(\frac{\pi x}{L}\right), \tag{2}$$

where L is the beam span. The deviation $\Delta y_{\text{str,u}}$ is illustrated in Fig. 3. Relatively long beam spans optimise the flexibility of the building; the combination of long spans and slender steel profiles may lead to the need of a bracing system at mid-span to prevent lateral-torsional buckling of the steel beam due to the self-weight of the large prefabricated concrete floor elements. The bracing system mitigates the out-of-straightness of the main girders, see Fig. 3. An out-of-straightness function compatible with the restraints imposed by the bracing at midspan is given by

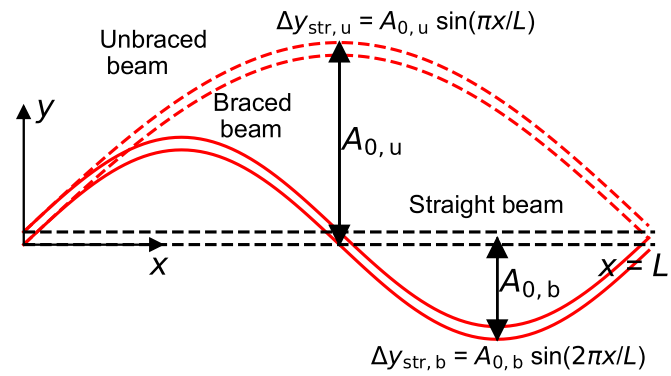

Fig. 3. Out-of-straightness of an unbraced beam and a beam braced at midspan compared to the nominal geometry (black).

Table 3
Maximum out-of-straightness amplitude $A_{o,u}$ for I and H sections.

Height h (mm)	Maximum out-of-straightness Hot rolled I/H sections [11]	Maximum out-of-straightness, beams in buildings [7]		
		Essential tolerance	Functional tolerance	
			Tolerance class 1	Tolerance class 2
$80 < h \le 180$	L/333	L/750	L/500	L/1000
$180 < h \le 360$	L/667			
$h > 360$	L/1000			

$$\Delta y_{\text{str,b}} = A_{0,b}\sin\left(\frac{2\pi x}{L}\right). \tag{3}$$

The length of the steel beam is not influenced by the bracing system. Therefore the arc length P of the sine wave is equal to the original beam length prior to execution. The arc length of the beam is given by

$$P = \int_0^L \sqrt{1 + \left(\frac{dy}{dx}\right)^2}\,\mathrm{d}x. \tag{4}$$

Eq. (4) indicates that the derivatives of Eqs. (2) and (3) must be equal to satisfy the requirement of equal arc length before and after execution. It follows that the amplitude of the out-of-straightness of the beam braced at midspan is one half of the amplitude of the out-of-straightness of the (original) unbraced beam, i.e. $A_{0,b} = 0.5{\cdot}A_{0,u}$. Similar derivations can be made for the case that the beam is braced at other locations along its span.

The out-of-straightness is limited by EN 10034 [11] for hot rolled sections and by EN 1090-2 [7] for all other profiles. An overview of the maximum out-of-straightness is given in Table 3.

The actual out-of-straightness of steel beams was extensively investigated in the context of establishing buckling curves in EN 1993-1-1 [12]. The average out-of-straightness of a large batch of various profiles (IPE, DIE, DIR, TB) determined by Beer & Schulz [13] is listed together with data found by Strating & Vos [14], Tebedge et al. [15], Dux & Kitipornchait [16], Aoki & Fukumoto [17] and Essa & Kennedy [18] in Table 4. The average out-of-straightness $A_{0,u}$ is L/2800 and the averaged standard deviation is L/5700. It is worth noticing that the experimental data presented in [13–18] originates from the 1970s to 1990s, and that technological advancements in the production process of steel beams may have decreased the magnitude of the out-of-straightness. The authors have inquired at various mills and workshops, but none actively registered the magnitude of the out-of-straightness,

Table 4
Out-of-straightness amplitude $A_{o,u}$ around the weak (z-)axis of various types of profiles.

Author	Profile	Number of specimens	Length (m)	Origin	Out-of-straightness $A_{0,u}$ (–)	
					Mean	Standard deviation
Beer & Schulz [13]	IAP 150 (IPE 140/160)			BE/GE	L/2100	
	IPE 160			NL	L/4400	
	IPE 200			BE	L/3800	
	DIE20 (HEA 200)			BE	L/3700	
	DIR20 (HEM 200)			BE	L/5800	
	Welded section			BE	L/5500	
Strating & Vos [14]	IPE 160		1.0–2.9	NL	L/1200	L/5000
Tebedge [15]	HEM 340	12	3.9–7.5	BE/DE/IT	L/3600	L/5800
Dux & Kitipornchait [16]	250UB37.3			AUS	L/2500	
Aoki & Fukumoto [17]	Welded H-section (100 × 100 mm)	85	1.4–2.9	JAP	L/3300	L/6400
Essa & Kennedy [18]	W360 × 39	11	9	CA	L/2000	–
Average					L/2800	L/5700

and therefore the deviations found in the 1970s–1990s are adopted in present work.

2.3. Relative displacement due to execution of the composite floor system

A relative displacement between the concrete floor elements and the steel beam occurs due to sliding of the floor elements relative to the steel beam because of their self-weight. This longitudinal relative displacement (slip) is assumed to be represented by a halve cosine wave [19] with amplitude s_0, according to

$$\Delta x_{\text{slip}} = -s_0 \cos\left(\frac{\pi x}{L}\right), \tag{5}$$

which is illustrated in Fig. 4.

The slip amplitude s_0 for a generic steel beam, symmetric with respect to midspan, on which prefabricated concrete floor elements with self-weight q_z per unit length are installed is

$$s_0 = \int_0^{L/2} \frac{1}{2}\frac{q_z x(L-x)e}{EI_0}\mathrm{d}x, \tag{6}$$

based on Euler-Bernoulli beam theory. In Eq. (6) e denotes the distance between the neutral axes of the steel beam and prefabricated concrete floor element, and EI_0 represents the bending stiffness without composite interaction. If the concrete floor elements are shorter than the beam span the bending stiffness EI_0 should be taken as the bending stiffness of the steel section. For prismatic steel beams, Eq. (6) reduces to

$$s_0 = \frac{1}{24}\frac{q_z L^3}{EI_0}e. \tag{7}$$

For non-prismatic steel beams, the evaluation of Eq. (6) is more complex than in case of a prismatic beam. To develop a simple approximation formula for the end-slip for non-prismatic steel beams, regression analysis is performed on the results obtained by solving the Euler-Bernoulli differential equation for beams subject to bending around their strong axis. The database of cross-sections that is considered consists of simply-supported web-tapered steel beams, symmetrical with respect to the plane at midspan, loaded by a uniformly distributed load q_z. It is assumed that the prefabricated concrete floor elements do not contribute to the bending resistance and have a height between 100 and 200 mm. The dimensional parameters considered in the database are listed in Table 5 and represent a wide range of bi-symmetrical and monosymmetrical steel beam designs, and therefore the approximation formula is considered to be generically applicable for this type of beam designs. Combining the parameters in Table 5 leads to 78,500 beam designs which are used as input for the regression analysis.

The approximate formula to determine the slip amplitude of a simply-supported web-tapered steel beam, symmetrical with respect to the plane at midspan, is determined based on the results obtained for the database of cross-sections as

$$s_0 = \frac{1}{24}\cdot\frac{q_z L^3}{0.35\cdot EI_0|_{x=0} + 0.65\cdot EI_0|_{x=L/2}}\cdot(0.2\cdot e|_{x=0} + 0.8\cdot e|_{x=L/2}). \tag{8}$$

The proposed approximation has a coefficient of determination (R^2) of 0.9998. The maximum deviations between the approximate formulae and the exact solution are +1.42% and −2.88%. In case of a prismatic beam, the approximation of Eq. (8) becomes the exact solution given by Eq. (7).

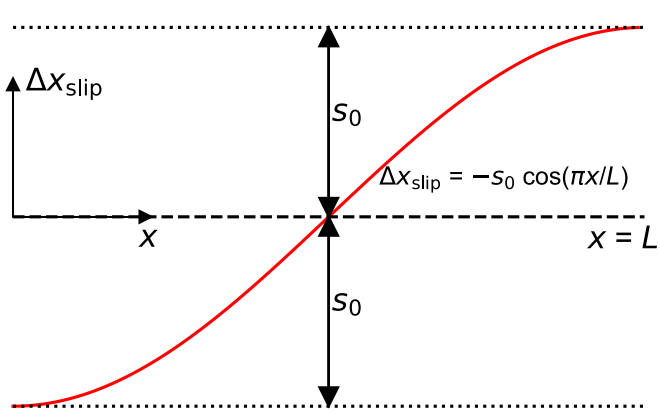

Fig. 4. Change in position of bolt hole occurring as a result of slip due to self-weight of the floor element.

2.4. Shear connector position within the floor element

It is assumed that a custom formwork is used to cast the prefabricated concrete floor elements, in which the demountable shear connectors are embedded. Such a formwork requires an investment, but leads to high-accuracy elements and increases fabrication speed. The

Table 5
Dimensional parameters considered in the derivation of an approximate formula for the end-slip of bi- and monosymmetrical non-prismatic beams.

Parameter	Physical meaning	Magnitude	Unit
L	Span	6, 8, 10, 12, 14, 16, 20	m
$h\|_{x\,=\,0,L}$	Beam height at supports	L/20, L/25, L/30	m
$\Delta h'$	Change in beam height per unit length	1.0%, 1.5%, 2.0%, 2.5%, 3.0%	–
b_f	Flange width	100, 150, 200, 250, 300	mm
$t_{f,t}$	Thickness of top flange	10, 12, 14, 16, 18	mm
$t_{b,t}$	Thickness of bottom flange	10, 12, 14, 16, 18	mm
t_w	Web thickness	4, 6, 8, 10, 12	mm

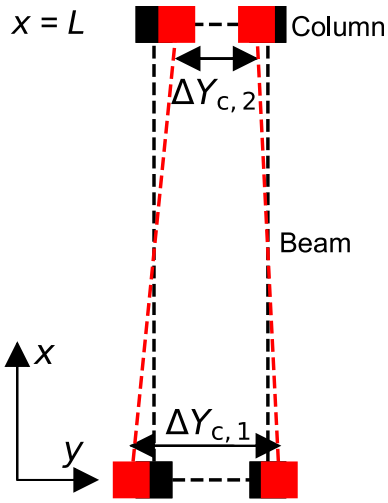

Fig. 5. Deviation between nominal (black) and actual distance (red) between adjacent beams at the supports, denoted by $\Delta Y_{c,1}$ and $\Delta Y_{c,2}$. (For interpretation of the references to colour in this figure legend, the reader is referred to the web version of this article.)

demountable shear connector is assumed to be fixed to the formwork with a nominal bolt-to-formwork clearance denoted by c_0. Due to the installation and tightening, the demountable shear connector will be in contact with the hole walls in nearly all cases and therefore c_0 can be regarded as a deterministic variable. The direction in which this occurs is random and is represented by the (random) angle ψ. The offset from the nominal position of the demountable shear connector is then given by

$$(\Delta x_{sc}, \Delta y_{sc}) = (c_0 \cos\psi, c_0 \sin\psi). \tag{9}$$

2.5. Column offset

The alignment of the demountable shear connectors embedded in the prefabricated concrete floor element and the bolt holes in the steel beam partially depends on the deviations of the structural grid. During the installation of the main and secondary steel beams part of the geometrical and dimensional deviations in the columns is corrected. However, the centre-to-centre distance between two adjacent beams may still vary. An overview of this deviation perpendicular to the span is illustrated in Fig. 5.

The magnitude of the deviation between the nominal distance between adjacent erected beams measured at the supports ($\Delta Y_{c,1}$ and $\Delta Y_{c,2}$) is limited by EN 1090-2 [7] as ± 10 mm and ± 5 mm for tolerance class 1 and 2, respectively. The maximum deviation for each individual erected beam end is not specified in EN 1090-2 [7], but can be approximated for $x = 0$ by

$$\Delta y_{c,1,L} = \eta_L \Delta Y_{c,1}; \;\; \Delta y_{c,1,R} = (1 - \eta_L)\Delta Y_{c,1}, \tag{10}$$

in which η_L is a random variable on the interval [0,1] and subscripts L and R denote the left and right beam, respectively. The deviation for the beams at $x = L$ can be modelled similarly. The deviation of the nominal position of the left beam in Fig. 5 is a function of position along the beam length described by the relation

$$\Delta y_c = \eta_L \Delta Y_{c,1} + (\eta_R \Delta Y_{c,2} - \eta_L \Delta Y_{c,1})\frac{x}{L}, \tag{11}$$

which is a linear interpolation function between the beam supports. A similar expression is derived for the right beam.

Column offset also exists in longitudinal direction, resulting in a staggered pattern of beams. For the two adjacent beams these random deviations are denoted as $\Delta X_{c,L}$ and $\Delta X_{c,R}$, respectively. Due to the axial rigidity of the steel beams the deviations are constant along their length, thus equally affecting the required nominal hole clearance of all demountable shear connectors.

2.6. The required nominal hole clearance

The total deviation from nominal positions in x and y directions of the bolt holes in the left steel beam in Fig. 5 and the centreline of the demountable shear connectors embedded in the concrete floor elements are given by Eqs. (12) and (13), respectively, based on Eqs. (1), (2), (3), (5), (9) and (11).

$$(\Delta x_{beam}, \Delta y_{beam}) = \left(R\cos\theta + \Delta X_{c,L}, R\sin\theta + A_{0,u/b}\sin\left(\frac{n_{u/b}\pi x}{L}\right) + \eta_L \Delta Y_{c,1} + (\eta_R \Delta Y_{c,2} - \eta_L \Delta Y_{c,1})\frac{x}{L}\right) \tag{12}$$

$$(\Delta x_{floor.}, \Delta y_{floor}) = \left(s_0 \cos\left(\frac{\pi x}{L}\right) + c_0 \cos\psi, c_0 \sin\psi\right). \tag{13}$$

Similarly the deviation is derived for the right beam. The magnitude of the distance between the actual centreline of the bolt hole and the actual centreline of the demountable shear connector, denoted by r, can be calculated using Pythagoras' theorem according to

$$r = \sqrt{(\Delta x_{beam} - \Delta x_{floor})^2 + (\Delta y_{beam} - \Delta y_{floor})^2}. \tag{14}$$

The demountable shear connector can be installed if

$$r + \frac{d}{2} < \frac{d_h}{2}, \tag{15}$$

in which d represents the nominal bolt diameter and d_h denotes the hole diameter. The required nominal hole clearance, defined as $d_h - d$, is equal to $2r$.

2.7. Statistical evaluation of required nominal hole clearance

EN 1090-2 [7] does not provide any details regarding the probability distribution of the geometrical and dimensional deviations. Kala [20] assumed that the deviations related to the out-of-straightness of beams are represented by a Gaussian (normal) distribution, and that 95% of all realisations fall within the imposed tolerance limitations. According to this approach, the tolerance limit represents a certain number of standard deviations, expressed as

$$n \cdot \sigma = |\pm \text{tolerance}|, \tag{16}$$

in which n is any natural number and equal to 1.96 for Kala's assumption. A smaller value of n implies that more observations outside the tolerances limits are expected. Kala's assumption is valid for all deviations, as long as the deviations are bilateral. In this paper, n is taken as 1.96, corresponding to 95% of the realisations complying to the tolerance limits.

Table 6 contains the statistical parameters that are assumed based on EN 1090-2 [7], Kala [20] andTable 4 for the normal-distributed basic variables in the performance function represented by Eq. (15). Tables 7 and 8 contain the uniformly distributed parameters and the deterministic variables, respectively.

The combination of different stochastic distributions is considered

Table 6
Normal-distributed basic variables.

Basic variable	Distribution	Mean	Tolerance Class 1 – Standard deviation	Tolerance Class 2 – Standard deviation	Unit
R	Normal	0	1.02	0.510	mm
$\Delta Y_{c,i}$	Normal	0	5.10	2.55	mm
$\Delta X_{c,i}$	Normal	0	5.10	2.55	mm
$A_{0,u}$	Normal	L/2800	L/5700	L/5700	–

Table 7
Uniformly-distributed basic variables.

Basic variable	Distribution	Interval	Unit
θ	Uniform	[0, 2π]	rad
ψ	Uniform	[0, 2π]	rad
η_i	Uniform	[0,1]	–

Table 8
Deterministic basic variables.

Basic variable	Distribution	Magnitude	Unit
s_0	Deterministic	Eq. (8)	mm
c_0	Deterministic	1	mm
d	Deterministic	e.g. 20	mm

using the Monte Carlo method. Random realisations of each of the basic variables as well as random positions along the length of the composite floor system are generated to evaluate the required nominal hole clearance (2r) based on Eq. (15). The aggregated results of the simulations are used to obtain the statistical distribution of the required nominal hole clearance. It is assumed that no correction of any deviations occurs during execution except for the installation of the bracing at midspan.

The successful application of demountable and reusable composite floor systems in engineering practice is influenced by the speed of execution, which is characterised by the ability to connect the demountable shear connector to the steel beams. The probability of successful installation of the demountable shear connector must therefore be sufficiently high, and depends on the risk the contractor is willing to take. For instance, it may be considered acceptable if 5 out of 100 prefabricated floor elements cannot be installed at the first attempted position. The 'failure' probability of 5% can then be used to determine the required nominal hole clearance by determining its 95th percentile value based on the aggregated simulation results.

2.8. A case-study building

The required nominal hole clearance is quantified for the case study of a main girder of a multi-storey car park building, with a design similar as in the experimental work of Nijgh et al. [4]. The composite floor system consists of web-tapered steel beams with a clear span of 16 m at a centre-to-centre distance of 2.7 m, and prefabricated concrete floor elements with a length of 8 m, a width of 2.7 m and a thickness of 0.12 m. The weight per unit length q_z of the prefabricated concrete floor elements is 8.1 kN/m. The steel beams and the prefabricated concrete floor elements are connected by demountable shear connectors embedded in the floor elements.

The height of the web-tapered steel beam varies linearly between the supports, $h|_{x=0,L} = 590$ mm, and midspan, $h|_{x=L/2} = 740$ mm. The thickness and width of the flanges, as well as the thickness of the web, are constant along the beam length and are provided in Fig. 6.

Tolerance classes 1 and 2 are considered in combination with the possible presence of a bracing system at midspan to prevent lateral-torsional buckling during execution. The out-of-straightness of the beam is assumed independent of the tolerance class as the statistical parameters originate from actual measurements (see Table 4) instead of from EN1090-2 [7]. The slip amplitude $s_0 = 2.96$ mm is determined based on Eq. (8).

The (stochastic) variables in Eqs. (12) and (13) are generated according to their distributions (Tables 6–8) followed by a deterministic evaluation of the performance function expressed by Eq. (15). The convergence of the statistical characteristics of the aggregated results is

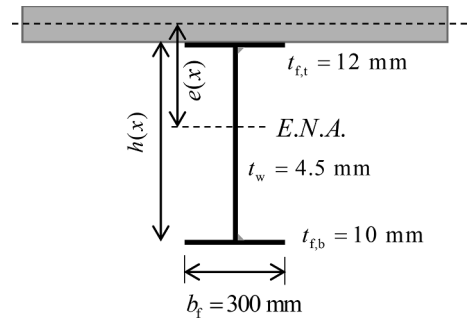

Fig. 6. Cross-section of the steel tapered beam, including prefabricated concrete floor element, considered in the case study.

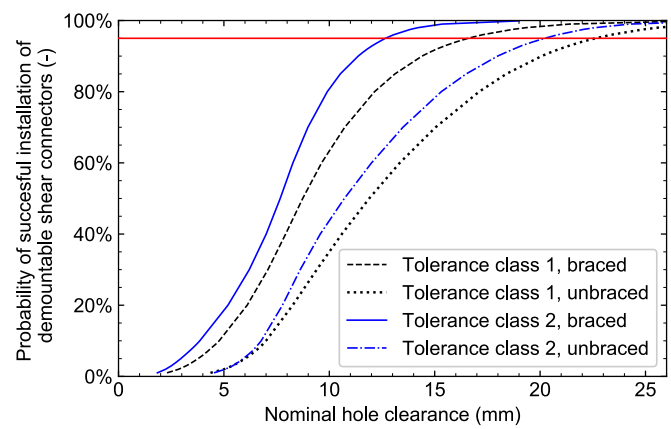

Fig. 7. Probability of successful installation of a demountable shear connector as a function of nominal hole clearance for the case study composite flooring system.

an indicator that sufficient number of simulations have been considered. For this case study the number of simulations is $N = 75{,}000$ based on a maximum deviation of the 95th percentile of the aggregated results between ten subsequent simulation runs of 0.05 mm.

The nominal hole clearance as a function of the probability of successful installation of the demountable shear connectors upon the first attempt is illustrated in Fig. 7. Because the demountable shear connectors embedded in a prefabricated concrete floor element should simultaneously align with the bolt holes in two beams, the joint probability P of alignment is

$$P(L \cap R) = P(L)P(R), \tag{17}$$

in which $P(L)$ and $P(R)$ denote the probability of individual alignment of the demountable shear connectors for the left and right beam, respectively.

The required nominal hole clearance for a given probability of successful alignment is smallest in case of tolerance class 2 in combination with a brace at midspan. In case of an unbraced span, the magnitude of the nominal hole clearance increases significantly for the same probability of successful installation of the demountable shear connectors. For a 95% probability of successful connector installation, a nominal hole clearance between 12.7 and 22.6 mm is necessary depending on the tolerance class and the bracing system.

Figs. 8 and 9 show a 'heat map' of the required nominal hole clearance for the successful installation of demountable shear connectors for the case study flooring system, with and without a bracing system, respectively. It can be observed that the critical locations to connect the demountable shear connectors are located at a quarter and at three-quarters of the span for a braced beam, which is in line with the out-of-straightness shape illustrated in Fig. 3. A similar trend is observed for the unbraced beam and indicates that the out-of-straightness

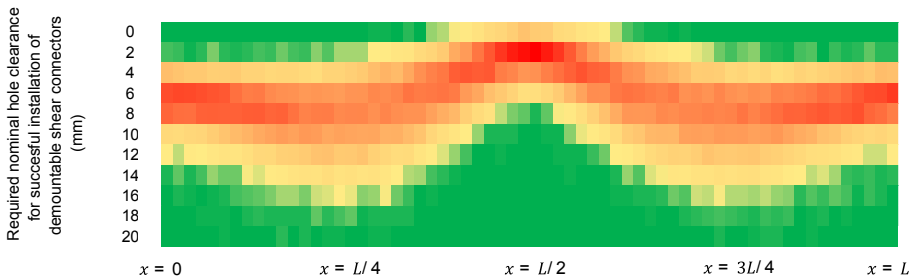

Fig. 8. Heat map identifying the need for a nominal hole clearance along the beam length for the case study composite floor system braced at midspan. Red denotes a high probability for a nominal hole clearance, green a low probability. (For interpretation of the references to colour in this figure legend, the reader is referred to the web version of this article.)

has a pronounced influence on the required nominal hole clearances.

It should be noted that the determination of the required nominal hole clearances is carried out under the assumption that it must be possible to connect the demountable shear connectors along the full length of the composite floor system. However, research has shown that concentrating the shear connectors near the supports is the most effective strategy to optimise the structural response of the composite beam [4,21]. Figs. 8 and 9 illustrate that at these locations the required nominal hole clearance is not maximum, implying that the current findings provide a lower bound probability of successful installation of the demountable shear connectors if they are concentrated in the support regions.

Nijgh et al. [4] successfully executed a steel-concrete composite floor system with similar specifications as mentioned in the above, using a 12 mm nominal hole clearance. However, the steel beams were braced at 5 locations during execution and the columns were not offset, leading to smaller required nominal hole clearances compared to the results of present analysis.

The results of the Monte Carlo analysis are based on the assumption that the floor elements do not exhibit geometrical and dimensional deviations. Gîrbacea [8] has identified the deviations in terms of longitudinal and transversal spacing of the embedded demountable shear connectors for the composite floor system executed by Nijgh et al. [4]. The maximum transversal deviations of the spacing of the demountable shear connectors were +2.6 and −2.8 mm. In longitudinal direction of the prefabricated concrete floor elements, the maximum deviations of the connector spacing were +1.4 and −0.9 mm. The floor elements were 4.8 mm too long on average. The observed deviations of the geometry and dimensions of the prefabricated concrete floor elements are significant, and arise due to a non-standardised production process and the use of steel angle profiles as formwork. A tight control over the dimensional and geometrical deviations of the prefabricated concrete floor elements would have mitigated the experimentally required nominal hole clearances. In addition, the floor elements could be designed slightly narrower than the nominal centre-to-centre distance of the steel beams to allow for minor deviations in floor element width [8]. This strategy cannot be used longitudinally, because direct contact of the floor elements is necessary to generate composite interaction during the functional lifetime.

2.9. Composite interaction

The significantly oversized holes facilitate a rapid execution process. As a consequence, they lead to a low probability of contact between the bolt and flange. This implies that composite interaction and its benefits, i.e. reduced deflection, increased resistance and a more favorable (higher) eigenfrequency, are not achieved unless the bolt-to-hole clearance is overcome. Therefore the need for oversized holes during the assembly and disassembly phase is contradicting the need for tight tolerances necessary to establish composite interaction during the functional lifetime. The aim of this section is to present an overview of how a rapid execution process can be effectively combined with composite interaction, and to provide an overview of the on-going research to modify existing design rules to be suitable for steel-concrete composite floor systems.

Two solutions are available to provide composite interaction without contact between bolt and flange, (i) preloading of the bolt such that the shear force is transferred by friction at the steel-concrete interface and (ii) injecting the bolt-to-hole clearance with an epoxy resin which transfers the load by bearing. One of the advantages of resin-injected connections is that the load-transfer mechanism does not depend on the condition of the faying surfaces. Nijgh et al. [4] used a resin-injected demountable shear connector, see Fig. 10, in a demountable and reusable steel-concrete composite floor system tested at Delft University of Technology to prove the feasibility of the technical solution for a multi-storey car park building. It was found that the application of resin-injected demountable shear connectors led to instantaneous composite action, without any sudden slip at increased load levels.

The design resistance of resin-injected bolted connections is specified in EN 1993-1-8 [22] for steel-to-steel double-lap shear connections, see Fig. 11, only. The design resistance of a non-preloaded resin-injected shear connector is the smallest value of the design shear resistance $F_{v,Rd}$ of the bolt and the design bearing resistance $F_{b,Rd,resin}$ of the resin. The bearing resistance of the resin can be calculated according to EN 1993-1-8 [22] as

$$F_{b,Rd,resin} = k_t k_s \beta \frac{d t_{b,resin} f_{b,resin}}{\gamma_{M4}}. \tag{18}$$

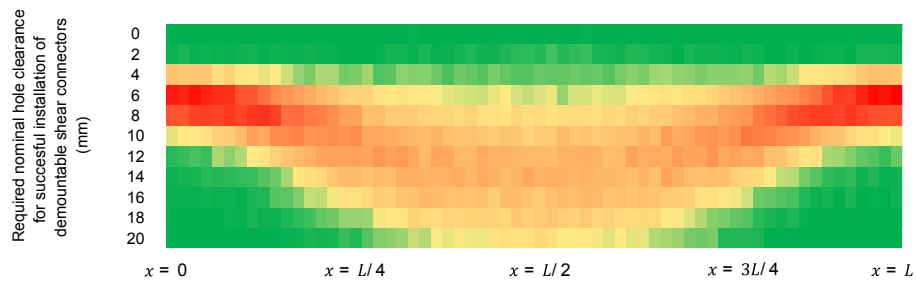

Fig. 9. Heat map identifying the need for a nominal hole clearance along the beam length for the unbraced case study composite floor system. Red denotes a high probability for a nominal hole clearance, green a low probability.

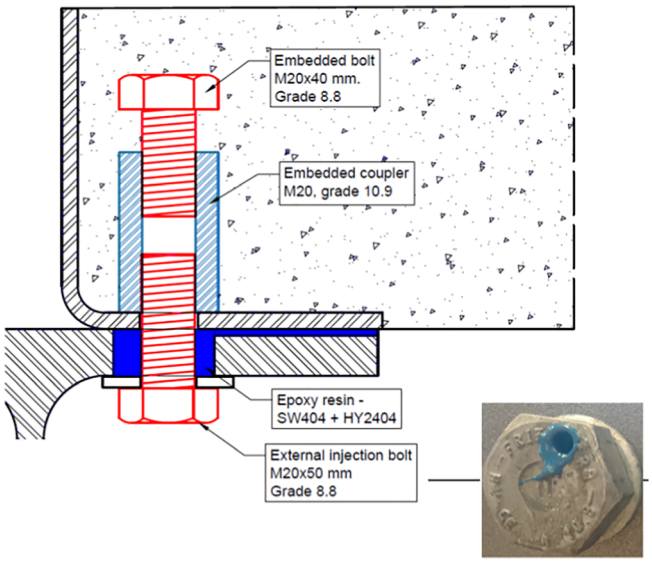

Fig. 10. Cross-section of a demountable shear connection with epoxy resin injected into the oversized bolt hole.

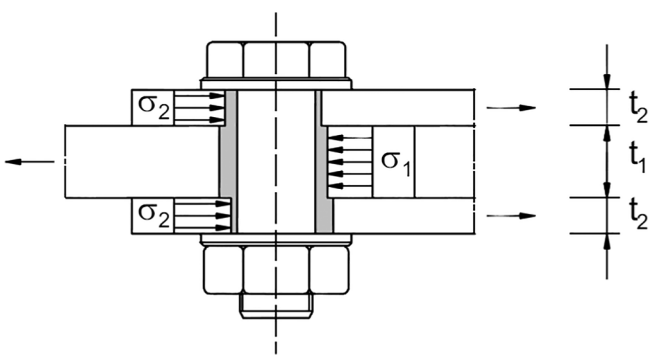

Fig. 11. Resin-injected steel-to-steel bolted shear connection according to EN 1993-1-8 [10].

Parameters β and $t_{b,resin}$ account for the influence of the ratios of the plate thicknesses on the deformation and the (potential) non-uniform bearing stress distribution due to the flexibility of the bolt, respectively [23]. Parameter k_t depends on the limit state considered, d denotes the bolt diameter, k_s takes account of oversized or slotted holes and $f_{b,resin}$ is the bearing strength of the resin determined in accordance with Annex K/G of EN 1090-2 [7]. Resin-injected bolted connections are recognised to be suitable for slip resistant connections [10]. Therefore, the procedure to determine $f_{b,resin}$ is based on a maximum relative displacement of the connected members (slip) of 0.30 mm after 50 years [7].

A set of creep tests is conducted to determine the bearing strength $f_{b,resin}$ as a function of the applied load level for single-lap shear connections with a large nominal hole clearance for the epoxy resin system SW 404 + HY2404/5159. The experiments are conducted using double-lap shear connections with $t_1 = 2t_2 = 20$mm with one bolt per connection. Only the hole in the centre plate is oversized (Ø32 mm) and the M20 bolts are located in the most unfavourable location with respect to the potential slip. The holes in the cover plates are normal-clearance holes against which the bolts are directly bearing to the steel plate to guarantee that only the time-dependent deformations caused by the epoxy resin in the centre plate are measured. The latter justifies the use of a double-lap shear connection to represent the behaviour of a single-lap shear connection used in steel-concrete composite floor systems, in which the resin is only present in the hole in the beam flange. The design of the creep specimens implies that β should be taken as unity and that $t_{b,resin}$ may be taken equal to thickness of the centre plate.

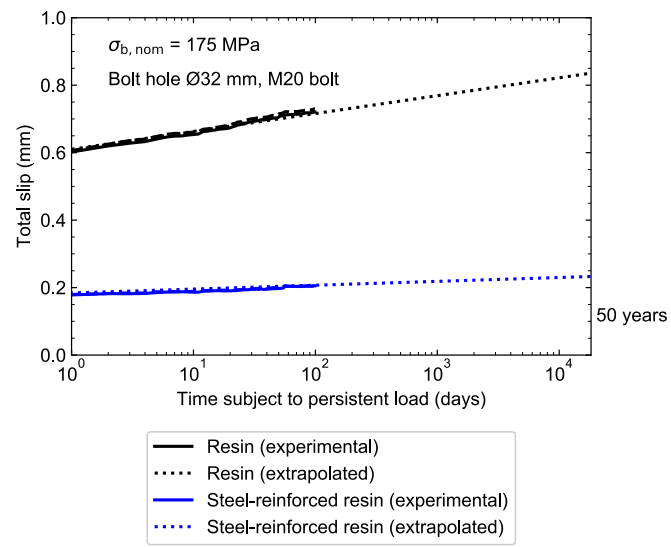

Fig. 12. Slip vs. time diagram for a double-lap shear connection with an M20 bolt and a (steel-reinforced) resin-injected oversized hole of Ø32 mm in the centre plate subject to a nominal bearing stress of 175 MPa.

Three nominal bearing stress levels; 125 MPa, 175 MPa and 225 MPa, are considered in on-going creep experiments at ambient temperature. The nominal bearing stress levels are held constant for a period of 100 days. The stress levels represent the range of $f_{b,resin}$ presented in literature [24–26] for double-lap shear connections with normal clearance holes.

The first creep test at a nominal bearing stress level of $\sigma_{b,nom} = 175$ MPa has been finalised. The results are shown in Fig. 12 and are the average of four nominally identical connections within the string of specimens. The experimental results are extrapolated on a semi-log diagram based on the provisions of EN 1090-2 [7]. The extrapolated slip of the resin-injected connections after 50 years is $\delta = 0.85$ mm. For a given deformation criterion δ_{max} (e.g. 0.30 mm after 50 years [7]) the bearing strength of the resin for this connection design is approximated by

$$f_{b,resin} = \frac{\min(\delta,\ \delta_{max})}{\delta} \cdot 175 = 62\ \text{MPa}. \tag{19}$$

Eq. (19) is recognised as conservative for $\delta_{max} < \delta$ because it assumes that the relation between deformation and bearing stress is linear. The effects of the epoxy resin layer thickness (dependent on the diameter of the bolt hole) is approximated by augmenting Eq. (19) as follows

$$f_{b,resin} = \frac{32 - 20}{d_h - d} \cdot \frac{\min(\delta_{max}, 0.85)}{0.85} \cdot 175\ \text{MPa}. \tag{20}$$

The term $(32–20)/(d_h - d)$ provides a linear correction for the nominal hole clearance, i.e. the "thickness" of resin in front of the bolt. This approximation is conservative for $d = 20$ mm and $d_h \geq 32$ mm because the bearing stresses spread laterally in larger bolt holes, leading to a lower effective bearing stress and therefore to smaller (time-dependent) deformations [27].

A novel material was recently developed as an alternative to the conventional epoxy resin and is referred to as steel-reinforced resin [27]. Steel-reinforced resin consists of a skeleton of steel spherical particles with a diameter of approximately 1 mm; the voids between the particles are filled using epoxy resin. This material exhibits a higher Young's Modulus [27–29] and smaller creep deformations [27] compared to the epoxy resin. The novel injection material is included in the testing program (with the same epoxy resin system to fill the voids) and the results are presented in Fig. 12. The performance of the steel-reinforced resin specimens is superior to that of the epoxy resin

specimens, with an extrapolated slip after 50 years of 0.24 mm, which is 30% of the deformation of the resin-injected connections. The steel-reinforced specimens comply with the current Eurocode slip criterion of 0.30 mm after 50 years and illustrate that an increase in the nominal hole clearance does not necessarily lead to a reduction in the bearing strength by choosing an appropriate injection material. Based on the same assumptions as for the epoxy resin, the bearing strength of the steel-reinforced resin is conservatively approximated by

$$f_{\mathrm{b,SRR}} = \frac{32-20}{d_{\mathrm{h}}-d}\cdot\frac{\min(\delta_{\max},\,0.24)}{0.24}\cdot 175\ \mathrm{MPa}. \tag{21}$$

Currently, the allowable slip after 50 years $\delta_{\max}$ does not depend on the field of application of the resin-injected bolted connection. The current slip limit is based on double-lap shear connections which transfer a tensile or compressive force between two members. A comparatively low slip limit is defendable for such connections, because the connection slip directly impacts the overall stiffness of the structural system. However, it could be argued that this limit might be too restrictive for statically loaded steel-to-concrete shear connections, because a reduction of the shear connector stiffness only leads to a comparatively negligible decrease of the effective bending stiffness (e.g. [30]). For steel-concrete composite floor systems, slip-mitigation therefore plays a larger role than slip-prevention, and for this reason the allowable slip criterion could be revised for this type of application. This would lead to an increase of the nominal bearing strength of the (steel-reinforced) epoxy resin.

The results of the pending experiments with a nominal stress range of 125 MPa and 225 MPa will be used to develop more comprehensive prediction models of the bearing strength of the (steel-reinforced) epoxy resin. In addition, the effect of the deformability of the bolt and the deformability of the epoxy resin will be considered separately to provide a more accurate representation of the effects of oversized holes on the bearing strength.

3. Conclusion

- The geometrical and dimensional deviations of a reusable composite floor system must be accounted for to facilitate easy and rapid execution. The deviations considered in present work include equations derived for column offset, bolt hole offset, shear connector offset, out-of-straightness and relative displacement (slip) between the steel beam and the prefabricated concrete floor elements due to their self-weight. The magnitude of the deviations has been identified based on EN 1090-2 [7] and literature. An approximate formula to quantify the slip for a composite girder consisting of prefabricated floor elements and a tapered steel beam has been derived based on regression analysis.
- A prediction model for the quantification of the required nominal hole clearance for a demountable shear connector for a composite floor system consisting of steel beams and large prefabricated concrete floor elements has been developed. The magnitude of the required nominal hole clearance mainly depends on span length, specified probability of successful installation of the demountable shear connectors, tolerance class and the presence of bracing systems. The prediction model has been applied to a tapered composite floor system, representing the main girder of a multi-storey car park building with a span of 16 m. For this case study example, a nominal hole clearance between 12.7 and 22.6 mm is required to achieve a 95% probability of successful installation of the prefabricated concrete floor elements, depending on the tolerance class and the bracing system.
- Composite interaction is achieved by injecting the large hole clearances with epoxy resin after execution, either with a commercial epoxy resin or a steel-reinforced resin. The bearing strength of the epoxy resin is defined as a function of relative displacement (slip) of the connected structural components. An approximate expression to determine the bearing strength of (steel-reinforced) epoxy resin SW404 + HY2404/5159 for use in steel-concrete composite floor systems is derived based on a 100-day creep test. The preliminary results of the on-going creep tests at different nominal stress ranges are used to develop comprehensive prediction models of the bearing strength of the (steel-reinforced) epoxy resin, taking into account the contributions of the deformability of the bolt and the deformability of the (steel-reinforced) epoxy resin. For the creep results presented in this paper, the connections with steel-reinforced epoxy resin show only 30% of the deformation obtained with the epoxy resin specimens.

Declaration of Competing Interest

The authors declare that they have no known competing financial interests or personal relationships that could have appeared to influence the work reported in this paper.

Acknowledgement

The first author gratefully acknowledges support by the Research Program of the Materials innovation institute (M2i) (www.m2i.nl), supported by the Dutch government, under project number T16045.

The second author gratefully acknowledges the financial support of the Research Fund for Coal and Steel (RFCS), within the research project “Reuse and Demountability using Steel Structures and the Circular Economy” REDUCE (RFCS-02-2015). Cooperation of the project partners (SCI, University of Luxembourg, University of Bradford, Lindab A/S, Tata Steel, Bouwen met Staal and AEC3) is gratefully acknowledged.

References

[1] Kozma A, Odenbreit C, Braun MV, Veljkovic M, Nijgh M. Push-out tests on demountable shear connectors of steel-concrete composite structures. Structures 2019;21:45–54.
[2] Pavlovic M, Veljkovic M. FE validation of push-out tests: using bolts as shear connectors. Steel Construct 2017;10(2):135–44.
[3] Suwaed ASH, Karavasilis TL. Removable shear connector for steel-concrete composite bridges. Steel Comp Struct 2018;29(1):107–23.
[4] Nijgh MP, Girbacea IA, Veljkovic M. Elastic behaviour of tapered composite beam optimized for reuse. Eng Struct 2019;183:366–74.
[5] Dobbelsteen A. The Sustainable Office – an exploration of the potential for factor 20 environmental improvement of office accommodation. Delft: Delft University of Technology; 2004.
[6] Tingly DD, Davinson B. Design for deconstruction and material reuse. Proc Inst Civ Eng 2011;164(EN4):195–204.
[7] NEN, EN1090-2: Execution of steel structures and aluminium structures – Part 2: technical requirements for steel structures, Delft: NEN, 2018.
[8] Girbacea IA. Assessment of demountable steel-concrete composite flooring systems. Delft: Delft University of Technology; 2018.
[9] E. Whitney, Manufacturing by Design, Harvard Business Review, no. 7, 1988.
[10] NEN, EN1993-1-8 – Eurocode 3: Design of steel structures – Part 1-8: Design of Joints, Delft: NEN, 2005.
[11] NEN, EN 10034: Structural steel I and H sections: Tolerances on shape and dimensions, Delft: NEN, 1993.
[12] NEN, En 1993-1-1. Eurocode 3: Design of steel structures - Part 1–1: General rules and rules for buildings. Delft: NEN; 2005.
[13] Beer H, Schulz G. The European Column Curves. In: Proceedings of the IABSE Colloqium on Column Strength, Paris; 1975.
[14] J. Strating and H. Vos, Computer Simulation of the E.C.C.S. Buckling Curve using a Monte-Carlo Method, Heron, vol. 19, no. 2; 1973.
[15] Tebedge N, Chen W, Tall L. Experimental studies on column strength of european heavy shapes. Bethlehem, Pennsylvania: Lehigh University; 1972.
[16] Dux PF, Kitipornchait S. Inelastic beam buckling experiments. J Constr Steel Res 1983;3(1):3–9.
[17] Aoki T, Fukumoto Y. On the buckling strength distribution of welded H-columns. In: Proceedings of the JSCE conference; 1974.
[18] Essa HS, Kennedy DJL. Distortional buckling of steel beams. Alberta: University of Alberta – Department of Civil Engineering; 1993.
[19] Lawson RM, Lam D, Aggelopoulos ES, Nellinger S. Serviceability performance of composite beams. Proc Inst Civ Eng 2017;170(SB2):98–114.
[20] Kala Z. Sensitivity analysis of steel plane frames with initial imperfections. Eng Struct 2011;33:2342–9.
[21] Zeng X, Jiang SF, Zhou D. Effect of shear connector layout on the behavior of steel-concrete composite beams with interface slip. Appl Sci 2019;9(1).
[22] European Committee for Standardization. NEN-EN 1993-1-8: design of steel

structures – part 1–8: design of joints. Delft: Nederlands Normalisatie Instituut; 2011.
[23] Bouwman LP. De invloed van de dikteverhoudingen van hoofd- en stuikplaten op de toelaatbare stuikspanning bij verbindingen met injectiebouten. Delft: Stevin-laboratorium van de afdeling der Weg-en Waterbouwkunde der Technische Hogeschool; 1974.
[24] Gresnigt AM, Beg D., Design bearing stresses for injection bolts with short and long duration high loads. In: Research and applications in structural engineering, mechanics and computation, Cape Town; 2013.
[25] Gresnigt A, Stark J. Design of bolted connections with injection bolts. In: Proceedings of the Third International Workshop - Connections in Steel Structures III, Trento; 1996.
[26] Gresnigt N, Sedlacek G, Paschen M. Injection bolts to repair old bridges. In: Proceedings of Connections in Steel Structures IV, Roanoke; 2000.
[27] Nijgh MP. New materials for injected bolted connections – a feasibility study for demountable connections. Delft: Delft University of Technology; 2017.
[28] Nijgh MP, Xin H, Veljkovic M. Non-linear hybrid homogenization method for steel-reinforced resin. Constr Build Mater 2018;182:324–33.
[29] Xin H, Nijgh MP, Veljkovic M. Computational homogenization simulation on steel-reinforced resin used in the injected bolted connections. Compos Struct 2019;210:942–57.
[30] Girhammar UA. A simplified analysis method for composite beams with interlayer slip. Int J Mech Sci 2009;51:515–30.